The interaction of IQGAP1 with the exocyst complex is required for tumor cell invasion downstream of Cdc42 and RhoA

Mika Sakurai-Yageta,[1,2] Chiara Recchi,[1,2] Gaëlle Le Dez,[1,2] Jean-Baptiste Sibarita,[1,2] Laurent Daviet,[3] Jacques Camonis,[1,4] Crislyn D'Souza-Schorey,[5,6] and Philippe Chavrier[1,2]

[1]Institut Curie, Centre de Recherche, Paris F-75248, France
[2]Centre National de la Recherche Scientifique, Unite Mixte Recherche 144, Paris F-75248, France
[3]Hybrigenics SA, Paris F-75014, France
[4]Institut National de la Santé et de la Recherche Médicale, Unite 528, Paris F-75248, France
[5]Department of Biological Sciences and [6]Walther Cancer Research Center, University of Notre Dame, Notre Dame, IN 46556

Invadopodia are actin-based membrane protrusions formed at contact sites between invasive tumor cells and the extracellular matrix with matrix proteolytic activity. Actin regulatory proteins participate in invadopodia formation, whereas matrix degradation requires metalloproteinases (MMPs) targeted to invadopodia. In this study, we show that the vesicle-tethering exocyst complex is required for matrix proteolysis and invasion of breast carcinoma cells. We demonstrate that the exocyst subunits Sec3 and Sec8 interact with the polarity protein IQGAP1 and that this interaction is triggered by active Cdc42 and

RhoA, which are essential for matrix degradation. Interaction between IQGAP1 and the exocyst is necessary for invadopodia activity because enhancement of matrix degradation induced by the expression of IQGAP1 is lost upon deletion of the exocyst-binding site. We further show that the exocyst and IQGAP1 are required for the accumulation of cell surface membrane type 1 MMP at invadopodia. Based on these results, we propose that invadopodia function in tumor cells relies on the coordination of cytoskeletal assembly and exocytosis downstream of Rho guanosine triphosphatases.

Introduction

Tumor cell invasion across tissue boundaries and metastasis are dependent on the capacity of cancer cells to breach the basement membrane, remodel the ECM, and migrate through the 3D matrix meshwork (Sahai, 2005; Yamaguchi et al., 2005b). One major route of invasion requires tumor cells to proteolytically cleave ECM and basement membrane components via a mechanism that is initiated by the formation of integrin-based cell/matrix contacts and involves matrix-degrading proteases (Friedl and Wolf, 2003). Metalloproteinases (MMPs), particularly membrane-type (MT) MMPs, including MT1-MMP, are

essential for pericellular proteolysis and tumor cell invasion (Deryugina and Quigley, 2006; Itoh and Seiki, 2006).

When analyzed on reconstituted ECM thin substrates, matrix degradation by invasive cells occurs at discrete sites corresponding to small (micrometer range) cellular protrusions at the ventral cell surface called invadopodia. Based on a substantial amount of work, invadopodia are currently viewed as dynamic extensions of the plasma membrane, where signaling components and cellular machineries involved in actin-driven membrane protrusion and exocytosis are thought to cooperate for delivering and concentrating integrins, active MMPs (MT1-MMP and MMP2), and other components at sites of contact with the ECM (Chen and Wang, 1999; Mueller et al., 1999; Hashimoto et al., 2004; McNiven et al., 2004; Tague et al., 2004; Yamaguchi et al., 2005a; Artym et al., 2006; Hotary et al., 2006). Invadopodia are thus thought to mimic the contact sites that form between tumor cells and the basement membrane during cell invasion (Friedl and Wolf, 2003; Buccione et al., 2004). Therefore, it is essential to understand how these structures can assemble into functional proteolytic invasive units.

M. Sakurai-Yageta and C. Recchi contributed equally to this paper.

Correspondence to Philippe Chavrier: philippe.chavrier@curie.fr

M. Sakurai-Yageta's present address is Division of Molecular Pathology, Dept. of Cancer Biology, Institute of Medical Science, University of Tokyo, Minato-ku, Tokyo 108-8639, Japan.

C. Recchi's present address is Molecular and Cellular Medicine, National Heart and Lung Institute, Imperial College London, London SW7 2AZ, UK.

Abbreviations used in this paper: F-actin, filamentous actin; MMP, metalloproteinase; MT, membrane type; WT, wild type.

The online version of this article contains supplemental material.

With the overall aim of identifying the machinery controlling invadopodia biogenesis and function, we found that the exocyst complex is a key component of invadopodial proteolysis and invasion of human breast adenocarcinoma cells. The exocyst complex, which consists of eight subunits, namely, Sec3, Sec5, Sec6, Sec8, Sec10, Sec15, Exo70, and Exo84, mediates the tethering of post-Golgi and endocytic recycling vesicles for targeted insertion at sites of active plasma membrane growth (Folsch et al., 2003; Prigent et al., 2003; Hsu et al., 2004). Genetic and cell biology studies in budding yeast, *Drosophila*, and mammals have shown that the exocyst complex is necessary for cellular functions that require polarized exocytosis to dynamic regions of the plasma membrane, such as budding in yeast, cell–cell adhesion, neurite and filopodia extension, and cell migration (TerBush et al., 1996; Grindstaff et al., 1998; Sugihara et al., 2002; Rosse et al., 2006). The current view is that the exocyst complex selects vesicles eligible for docking by recognizing molecular codes such as GTPases of the Rab subfamily on the incoming vesicles and assembles in a vesicle-tethering complex at specialized regions of the plasma membrane that are delineated by small GTPases belonging to the Rho family and to the Ral and ADP-ribosylation factor subgroups (Munson and Novick, 2006).

In this paper, we identify new exocyst complex partners and/or regulators that play a role in tumor cell invasion. We show that the Sec8 and Sec3 subunits interact with the cell polarization landmark IQGAP1 (Noritake et al., 2005; Brown and Sacks, 2006) and that this interaction is controlled by the Rho GTPases Cdc42 and RhoA. We also provide an indication that this association is involved in matrix degradation in highly invasive MDA-MB-231 human breast carcinoma cells. Overall, our study identifies novel components of the exocytic machinery acting downstream of Cdc42/RhoA GTPases that are essential for the formation and activity of invadopodia in breast tumor cells.

Results

The exocyst complex is required for breast tumor cell invasion

MDA-MB-231 breast tumor cells are known to degrade the matrix at invadopodia through a mechanism dependent on MMP activity (Sabeh et al., 2004). We first investigated the contribution of the exocyst complex to invadopodial matrix proteolysis of MDA-MB-231 cells, as the exocyst controls the docking of transport vesicles to dynamic exocytic sites at the plasma membrane, a definition that complies with invadopodial features.

To initiate these studies, the effect of knocking down MT1-MMP using a specific siRNA duplex was analyzed in MDA-MB-231 cells stably transfected with a fluorescent mCherry-tagged MT1-MMP construct (MDA-MT1ch cells; Fig. 1 a, top) or in the parental cell line. Reduction of MT1-MMP expression abolished matrix proteolysis of both MDA-MT1ch (Fig. 1 b) and MDA-MB-231 cells (Fig. S5, available at http://www.jcb.org/cgi/content/full/jcb.200709076/DC1), confirming that MT1-MMP is central to ECM degradation (Ueda et al., 2003; Sabeh et al., 2004; Artym et al., 2006). Knocking down Sec6, Sec8, or Sec10 exocyst complex subunits to 5–40% of their normal levels using

two independent siRNAs for each of the exocyst subunits (Fig. 1 a) resulted in a 50–65% inhibition of matrix degradation as compared with control MDA-MT1ch cells (Fig. 1, b and c). Similar results were observed upon depletion of the exocyst (Sec8) in parental MDA-MB-231 cells (see Fig. 5). These observations suggested that the exocyst complex contributes to invadopodial degradation of breast tumor cells.

To investigate whether the reduced pericellular proteolytic activity observed on depletion of some exocyst components correlated with a decreased capacity of MDA-MB-231 cells to invade across the ECM, we used a transwell chamber invasion assay using matrigel as the barrier to invasion. Loss of function of the exocyst complex by siRNA reduced invasion of MDA-MB-231 cells to 40–60% of control cells, depending on the exocyst subunit targeted for knockdown (Fig. 1 d). All together, these findings demonstrate that the exocyst complex is a key element in the mechanism of invasion of breast carcinoma cells.

Sec3 and Sec8 associates with IQGAP1 in vitro

Using a yeast two-hybrid assay, we identified the closely related IQGAP1 and IQGAP2 proteins as potential binding partners of Sec3, Sec8, Exo70, and Exo84 (Fig. S1, available at http://www.jcb.org/cgi/content/full/jcb.200709076/DC1). IQGAP1, a Cdc42 and Rac effector protein that regulates cell polarization during migration (Noritake et al., 2005; Brown and Sacks, 2006), has been recently implicated in invasion and metastasis (Clark et al., 2000; Nabeshima et al., 2002; Mataraza et al., 2003; Jadeski et al., 2008). As we did not detect the expression of IQGAP2 in MDA-MB-231 cells (unpublished data), our further analyses focused on IQGAP1.

The two-hybrid interactions defined a conserved region of the C-terminal end of IQGAP1 and IQGAP2 (57% identity) as the putative binding site for the exocyst subunits (Fig. S1, a and b). Thus, we performed in vitro GST pull-down assays from lysates of HeLa cells transfected with HA-tagged Sec3, Sec8, Exo70, or Exo84 exocyst complex subunit. The C-terminal end of IQGAP1 (position 1,361–1,657, IQGAP1-CTer1; Fig. 2 a) and a subregion (position 1,361–1,563, Cter2) comprising a predicted coiled-coil domain fused to GST specifically recovered all four exocyst subunits (Fig. 2 b). In contrast, the coiled-coil domain (position 1,491–1,538, Cter4) was not sufficient for binding on its own, nor was the far-most C-terminal fragment (1,563–1,657, CTer3). Interaction of the exocyst subunits with the coiled-coil–containing region of IQGAP1 was specific, as no such interaction could be detected between Sec8 and the predicted coiled-coil domain of the JSAP1/JIP3 scaffolding protein (Fig. S2 a, available at http://www.jcb.org/cgi/content/full/jcb.200709076/DC1; Kelkar et al., 2000).

To further clarify the interaction of IQGAP1 with the exocyst complex, pull-down assays were performed in cells depleted in the Sec3 and/or Sec8 subunits. Combined knockdown of Sec3 and Sec8 with specific siRNAs, although affecting the expression level of HA-Exo70 to some extent (43% reduction as compared with mock-treated cells; Fig. 2 c, top; compare lane 1 with lane 4), led to a strong reduction of HA-Exo70 binding to the IQGAP1 CTer2 fragment (Fig. 2 c, top; compare lane 6 with lane 12).
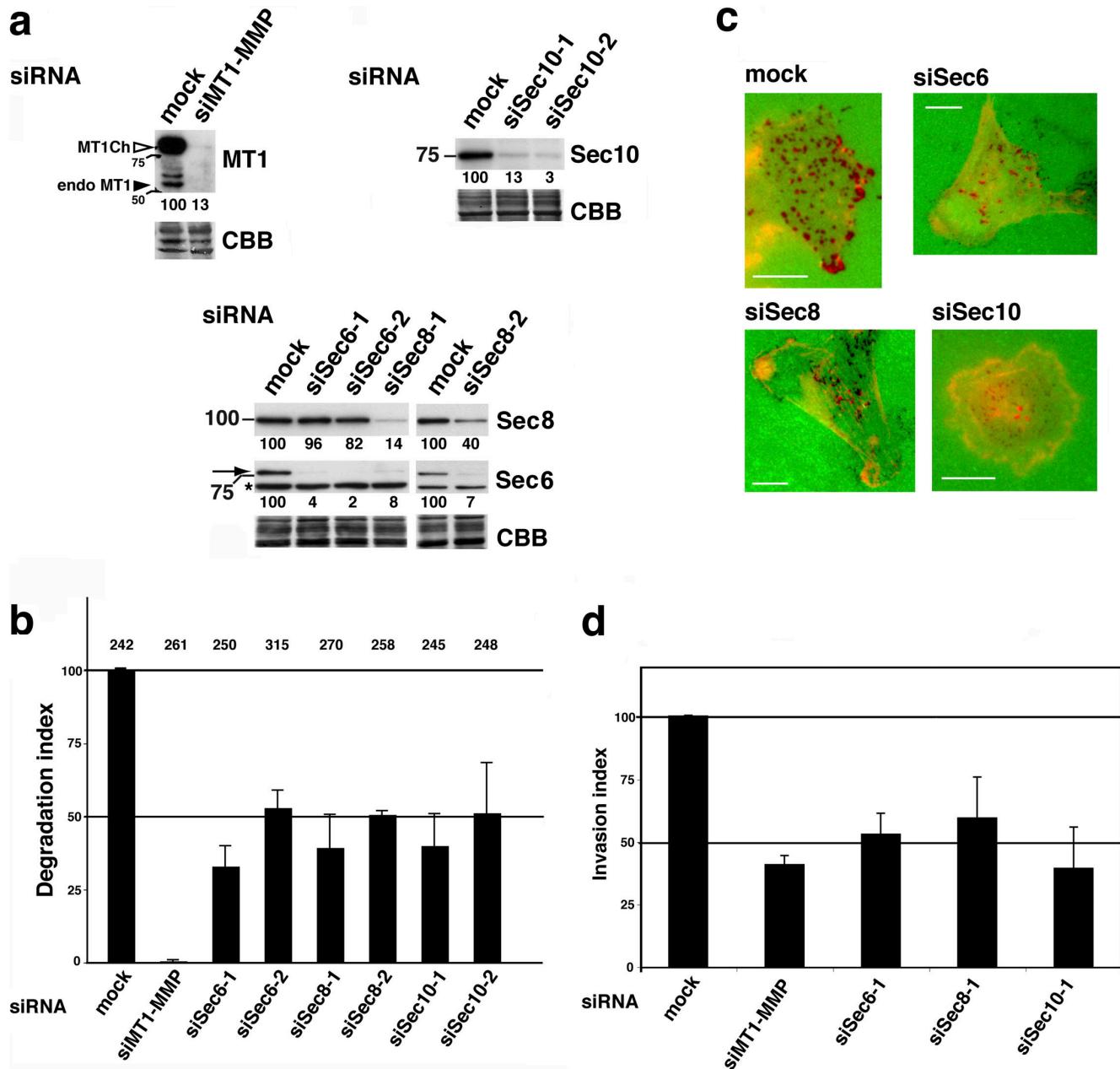
Figure 1. **The knockdown of exocyst complex subunits inhibits matrix degradation and invasion of breast cancer cells.** (a) The expression levels of MT1-MMP (MT1), Sec6, Sec8, and Sec10 were analyzed by immunoblotting with specific antibodies in lysates of MDA-MT1ch cells (i.e., MDA-MB-231 cells stably transfected with a construct encoding mCherry-tagged MT1-MMP) treated with the indicated siRNAs for 72 h. After immunoblotting, membranes were stained with Coomassie Brilliant blue (CBB) to control for equal loading. The open arrowhead indicates the position of mCherry-tagged MT1-MMP (MT1Ch). The closed arrowhead points to a processed, catalytically active (60 kD) form of endogenous MT1-MMP (endo MT1). Of note, depletion of the Sec8 exocyst complex subunit led to a reduction of the Sec6 level (arrow). Residual levels of knocked down proteins, as calculated based on densitometric analysis of Western blots, are indicated underneath the blots with respect to the level of mock-treated cells set to 100. The asterisk indicates a nonspecific band detected with anti-Sec6 antibodies that was not depleted upon treatment with Sec6 siRNAs. Molecular masses are indicated in kilodaltons. (b) Effect of MT1-MMP and exocyst subunit-specific siRNAs on the capacity of MDA-MT1ch cells to degrade fluorescent gelatin. MDA-MT1ch cells treated with the indicated siRNAs for 72 h were further incubated on FITC-gelatin for 4 h. Then, cells were fixed and stained with fluorescent phalloidin to label F-actin in all cells. Data are represented as normalized degradation (degradation index), which was calculated as the area of degraded matrix per cell relative to mock-treated cells (mean percentage ± SEM [error bars]) from at least three independent experiments with two coverslips each. The number of cells analyzed for each siRNA is indicated above the bars. (c) Representative images of MDA-MT1ch cells treated with the indicated siRNA and cultured on FITC-gelatin for 4 h. Merged images of F-actin (red) and gelatin (green) are shown. Bars, 10 µm. (d) Effect of MT1-MMP and exocyst subunit-specific siRNAs on the capacity of parental MDA-MB-231 cells to cross a layer of matrigel in a transwell chamber. Data are represented as normalized invasion (invasion index) relative to mock-treated cells calculated as described in Materials and methods (mean percentage ± SEM; each siRNA-treated cell population was analyzed in triplicate in at least three independent experiments).

In addition, single Sec3 or Sec8 knockdown also resulted in decreased binding of Exo70 to GST-IQGAP1/CTer2 (Fig. 2 c, compare lanes 6, 8, and 10). Furthermore, we observed that when the exocyst subunits were in vitro translated in reticulocyte lysates, only Sec3 and Sec8 but not Exo70 or Exo84 bound the IQGAP1 CTer1 and CTer2 constructs (Fig. S2 c). All together, these findings
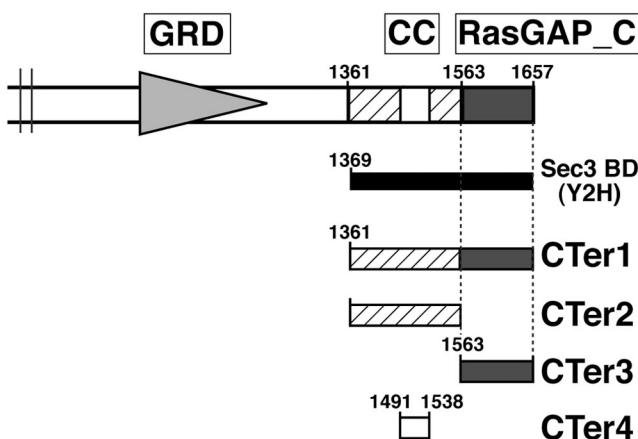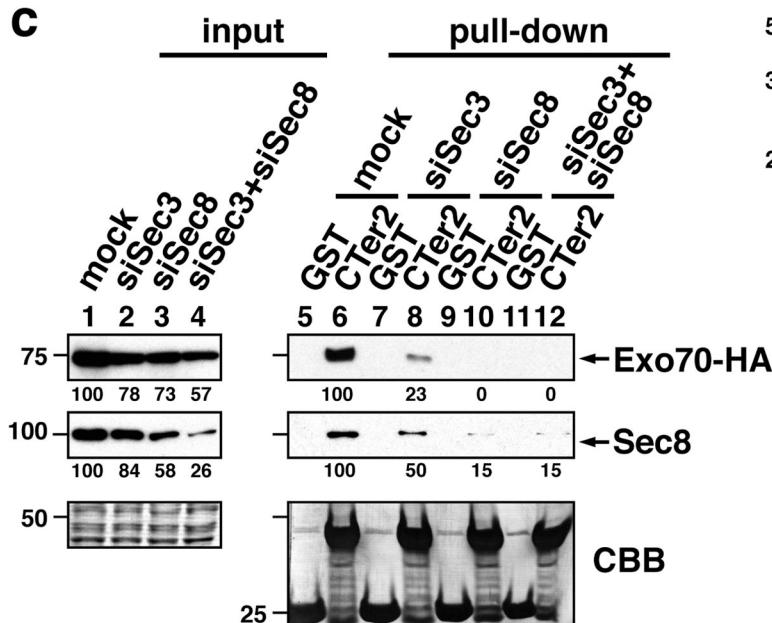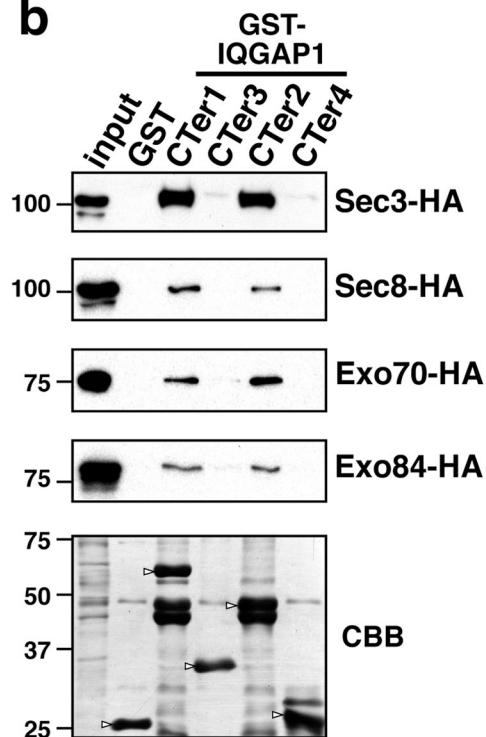
Figure 2. **Sec3 and Sec8 exocyst complex subunits interact with a C-terminal region of IQGAP1.** (a) Schematic representation of the C-terminal fragments of human IQGAP1 used. GRD, Ras GTPase-activating protein–related domain (binding site for GTP-Rac1/Cdc42); CC, coiled-coil domain predicted by COILS (version 2.2); RasGAP_C, RasGAP C terminus; Sec3 BD, minimal overlapping region of nine independent IQGAP1 clones isolated in a yeast two-hybrid screen using human Sec3 as bait (Fig. S1, available at http://www.jcb.org/cgi/content/full/jcb.200709076/DC1). (b) Lysates of HeLa cells transfected with HA-tagged human Sec3, Sec8, Exo70, or Exo84 were incubated with the indicated C-terminal fragment of IQGAP1 fused with GST immobilized on beads, and bound proteins were analyzed by immunoblotting with anti-HA antibody. 1% of lysates was loaded as a control (input). The bottom panel shows the different GST-IQGAP1 fragments separated by SDS-PAGE and stained with Coomassie Brilliant blue (CBB). Arrowheads indicate intact GST fusion proteins. (c) Effect of Sec3/Sec8 depletion on binding of the exocyst to IQGAP1-CTer2. HeLa cells were treated for 48 h with Sec3- or Sec8-specific siRNA alone or in combination as indicated and were further transfected with a construct encoding HA-tagged human Exo70 for 18 h. Lysates were prepared and incubated with GST-IQGAP1-CTer2, and bound proteins were analyzed by immunoblotting with anti-HA (top) or anti-Sec8 (middle) antibodies. The bottom panel shows GST and GST-IQGAP1-CTer2 proteins separated by SDS-PAGE and stained with Coomassie Brilliant blue. Residual levels of knocked down proteins and of proteins bound to GST-IQGAP1/CTer2 are indicated underneath the blots with respect to the level of mock-treated cells based on densitometric analysis. The efficiency of Sec3 depletion with siSec3 is documented in Fig. S2 b. Molecular masses are indicated in kilodaltons.

suggest a direct, possibly cooperative binding of Sec3 and Sec8 to the C-terminal region of IQGAP1. On the contrary, association of the other exocyst subunits, including Exo70 and Exo84, might be indirect, requiring Sec3/Sec8 bound to IQGAP1.

To map the IQGAP1-binding region of Sec3 and Sec8 subunits, several fragments of these proteins were translated in vitro and tested for binding to the GST-CTer2 construct of IQGAP1

(see Fig. S2 d for a schematic representation of the Sec3/Sec8 fragments used). This analysis identified predicted coiled-coil domains present at the N terminus of Sec3 and Sec8 as the IQGAP1-binding region (Fig. S2 e). Confirming previous results (Matern et al., 2001), our two-hybrid screens also documented reciprocal interactions of Sec3 and Sec8 through their predicted N-terminal coiled-coil domains (unpublished data). Collectively,

a

IP:

b

IP: Anti-GFP IP | input

c

d
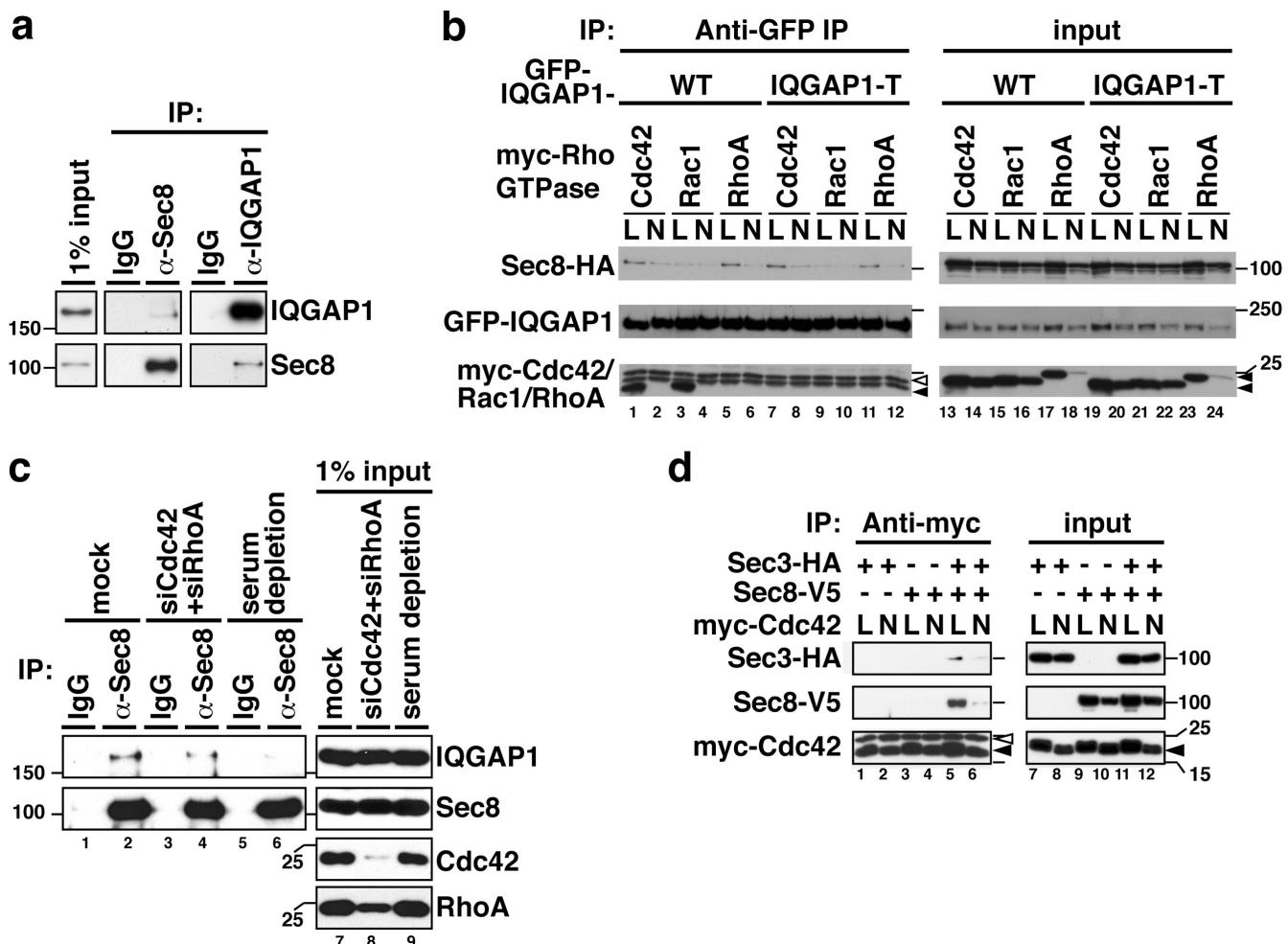
Figure 3. In vivo interaction of IQGAP1 with Sec8 and Sec3 is regulated by Cdc42 and RhoA. (a) Endogenous association of IQGAP1 with Sec8 in MD-MB-231 cells. 2 mg lysates of MDA-MB-231 cells was immunoprecipitated with control, anti-Sec8, or anti-IQGAP1 IgGs, and bound proteins were analyzed by immunoblotting with the indicated antibodies. 1% of total lysate was loaded as a control (input). Densitometric analysis showed that ∼2% of immunoprecipitated Sec8 was in complex with IQGAP1, and ∼7% of immunoprecipitated IQGAP1 was associated with Sec8 in typical experiments. (b) Activated Cdc42 and RhoA promote IQGAP1 association with Sec8 in transfected HEK293 cells. HA-tagged Sec8 was transiently coexpressed with GFP-tagged wild-type (WT) or mutant IQGAP1-T1050AX2 (IQGAP1-T) in HEK293 cells together with myc-tagged Cdc42, Rac1, or RhoA GTPases either in their GTP-bound form (L [Cdc42-Q61L], Rac1-Q61L, or RhoA-Q63L) or GDP-bound form (N [Cdc42-T17N], Rac1-T17N, or RhoA-T19N). IQGAP1-T harbors mutations in the GRD domain that abolish binding to GTP-Cdc42/Rac1 (Fukata et al., 2002). Approximately 1 mg of cellular extract was immuno-precipitated with anti-GFP antibodies and analyzed by anti-HA (top), anti-GFP (middle), or anti-myc (bottom) immunoblotting as indicated (lanes 1–12). Control IPs with irrelevant IgGs are shown in Fig. S3 b. Protein expression levels in 10 µg of total cell extracts are shown in the right panel (input, lanes 13–24). Of note, mycRhoA-T19N was consistently expressed to a lower extent as compared with mycRhoA-Q63L. The open arrowhead indicates the position of IgG light chain, and closed arrowheads point to myc-tagged Rho GTPases. (c) Cdc42 and RhoA activities are required for IQGAP1–Sec8 complex formation in MDA-MB-231 cells. The same amount of cell lysates prepared from MDA-MB-231 cells either mock treated (lanes 1 and 2), depleted for 72 h with combined siRNAs for Cdc42 and RhoA (lanes 3 and 4), or serum starved for 48 h (lanes 5 and 6) were immunoprecipitated with control IgGs or anti-Sec8 antibodies, and bound proteins were analyzed by immunoblotting with the indicated antibodies. A fraction (1%) of the lysates was analyzed as a control (input, lanes 7–9). (d) Sec3 and Sec8 form a complex with and dependent on GTP-bound Cdc42. HEK293 cells were transiently transfected with HA-tagged Sec3, V5-tagged Sec8, and myc-tagged Cdc42-Q61L (L) or -T17N (N) as indicated, and ∼1 mg of cellular extracts was immunoprecipitated with anti-myc antibodies (lanes 1–6). Bound proteins were analyzed by anti-HA, anti-V5, and anti-myc immunoblotting as indicated. Protein expression levels in 10 µg of total cell extracts are shown in the right panel (input, lanes 7–12). The open arrowheads indicate IgG light chain, and closed arrowheads indicate myc-tagged Cdc42. Control IPs with irrelevant IgGs are shown in Fig. S3 c (available at http://www.jcb.org/cgi/content/full/jcb.200709076/DC1). Molecular masses are indicated in kilodaltons.

these results indicate that Sec3, Sec8, and IQGAP1 can associate through coiled-coil domains present in all three proteins.

A GTP-Cdc42/RhoA-triggered association of Sec3/Sec8 with IQGAP1

Then, we investigated the interaction between the exocyst complex and IQGAP1 in vivo. First, we analyzed the association of endogenous IQGAP1 with the exocyst complex in MDA-MB-

231 cells. Low levels of IQGAP1–Sec8 complexes were repro-ducibly detected in reciprocal coimmunoprecipitations from MDA-MB-231 cell lysates (Fig. 3 a), which is indicative of an association of IQGAP1 with the exocyst complex in these cells. To examine the regulation of the IQGAP1–exocyst complex in further detail, epitope-tagged proteins were transfected into HEK293 cells, wherein transfection efficiency was high and protein association was better monitored. We first verified that

Figure 4. **Localization of IQGAP1 and Sec8 at F-actin–rich invadopodia in MDA-MB-231 cells plated on cross-linked fluorescent gelatin.** (a) MDA-MB-231 cells were plated on fluorescent FITC-gelatin, and, after 5 h, cells were fixed and stained for immunofluorescence microscopy with anti-IQGAP1 antibodies and fluorescent phalloidin. F-actin and endogenous IQGAP1 colocalize at invadopodia corresponding to proteolytic holes in the fluorescent gelatin matrix (right). (b) Phalloidin and anti-V5 staining of MDA-MB-231 cells transiently expressing V5-tagged Sec8 after 5 h on FITC-gelatin showing colocalization of F-actin and overexpressed Sec8 at invadopodia. (c) MDA-MB-231 cells transiently transfected with V5-tagged Sec8 together with HA–MT1-MMP and Y527F c-Src were plated for 4 h on AlexaFluor350-gelatin and stained for immunofluorescence microscopy with the indicated antibodies. Higher magnification views of the boxed areas are shown underneath each image. Bars, 10 µm.
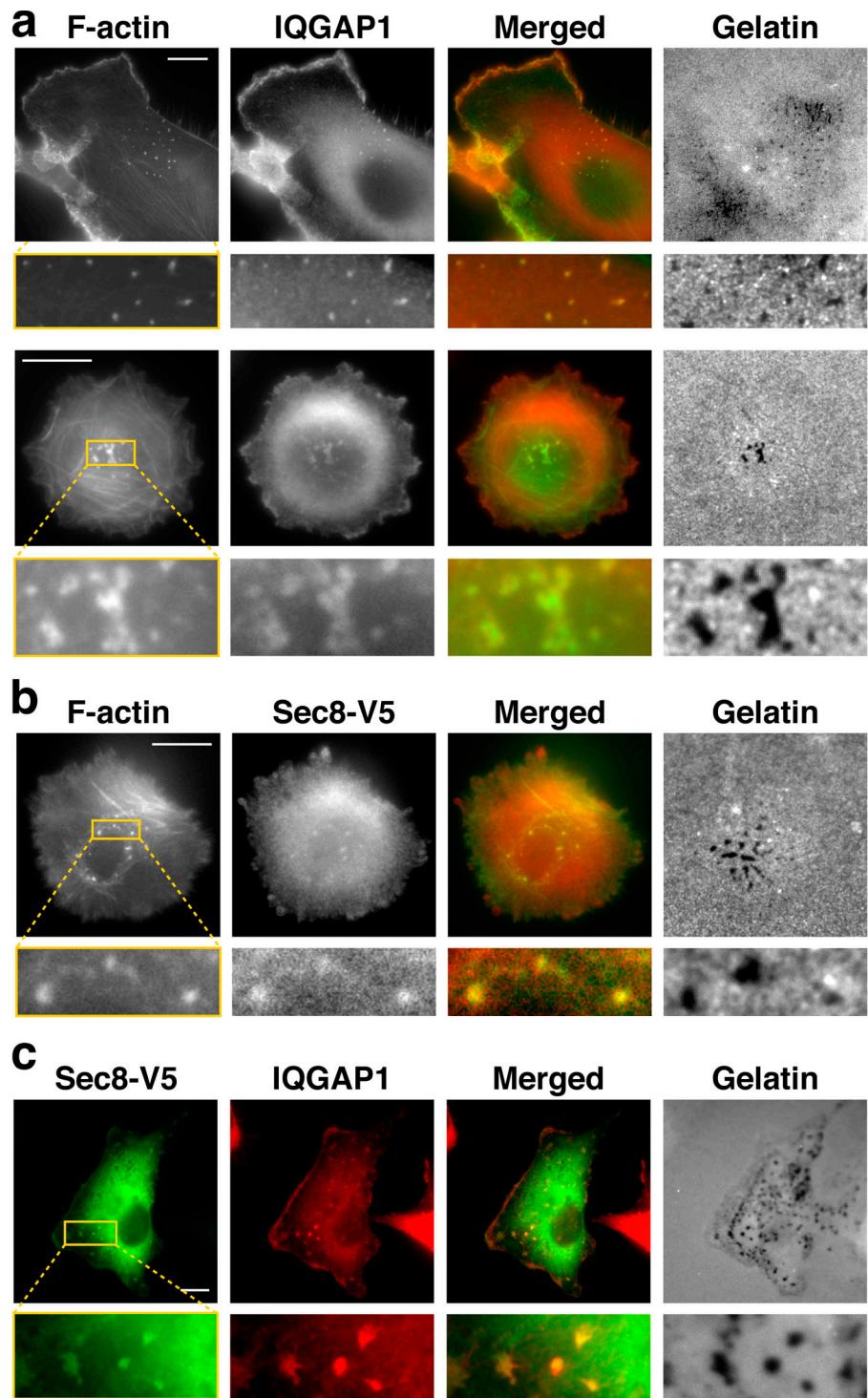
HA-tagged Sec8 and Sec3 were functional and interacted with endogenous Sec6 and Sec10 subunits by coimmunoprecipitation analysis (unpublished data). Because IQGAP1 is a known effector of Cdc42 and Rac1 small GTPases, HEK293 cells were transfected with constructs encoding wild-type (WT) IQGAP1 (tagged with GFP), Sec8-HA, and either constitutively active (Q to L substitution at position 61 or 63) or dominant inhibitory (T to N substitution at position 17 or 19) mutant forms of myc-tagged Cdc42, Rac1, or RhoA, and the interaction of IQGAP1 with Sec8 and Rho GTPases was analyzed by immunoprecipita-tion with anti-GFP antibodies. As previously shown, WT IQGAP1 interacted specifically with the GTP-bound form of Cdc42 and Rac1 but not RhoA (Fig. 3 b, bottom; compare lanes 1, 3 and 5, respectively; Noritake et al., 2005). On analyzing the presence of Sec8-HA in the immunoprecipitates, we made the observation that active Cdc42 and RhoA but not Rac1 promoted the association of IQGAP1 with Sec8 (Fig. 3 b, top; compare lanes 1, 5, and 3). Similarly, active Cdc42 induced the associa-tion of IQGAP1 with Sec3-HA (Fig. S3 a, lane 7; available at http://www.jcb.org/cgi/content/full/jcb.200709076/DC1).

When cells were transfected with a mutant of IQGAP1, IQGAP1-T1052AX2 (IQGAP1-T), which was shown to be defective for binding to Cdc42/Rac1 (Fukata et al., 2002), none of the Rho GTPases were found to interact with IQGAP1-T (Fig. 3 b, bottom; lanes 7–12). However, the binding of mutant IQGAP1-T to Sec8 was observed upon coexpression of the active form of Cdc42 or RhoA, whereas Rac1 was unable to promote this interaction (Fig. 3 b, top; lanes 7 and 11).

We also analyzed the consequence of the loss of Cdc42/RhoA activity on endogenous association of IQGAP1 with Sec8 in MDA-MB-231 cells. Serum starvation of MDA-MB-231, a treatment known to cause a reduction of active Cdc42 and RhoA levels in various cell types (Ren and Schwartz, 2000), led to an ∼80% reduction (±22%; from two independent experiments) of the steady-state association of IQGAP1 with Sec8 (Fig. 3 c, compare lane 2 with lane 6). In addition, reduced expression of Cdc42 and RhoA upon siRNA treatment also reduced the amount of IQGAP1 coimmunoprecipitated with Sec8 (43 ± 16% reduction as compared with mock; Fig. 3 c, compare lane 2 with lane 4).

Based on the aforementioned results, we conclude that although GTP-bound Cdc42 and RhoA can promote the association of IQGAP1 with the Sec8/Sec3 subunits of the exocyst complex in vivo, direct binding of these Rho GTPases to IQGAP1 is not required for this effect. Thus, we tested the possibility that active Cdc42/RhoA might interact with the exocyst subunits and, thus, facilitate their association with IQGAP1. When HEK293 cells were transfected with active or inactive Cdc42 together with Sec3-HA and Sec8-V5, active myc-Cdc42 was coimmunoprecipitated with both Sec3 and Sec8, and these interactions were detected only on coexpression of the two exocyst subunits (Fig. 3 d, top and middle; lane 5). A complex of active RhoA with Sec3/Sec8 was also detected, although to a lower extent (Fig. S3 d). The interaction of GTP-bound Cdc42 and RhoA with the exocyst subunits is probably transient in nature and can be detected only upon direct immunoprecipitation of the myc-tagged Rho GTPases when both Sec3 and Sec8 subunits are overexpressed (compare situations documented in Fig. 3, b and d). Collectively, our results suggest that upon activation (i.e., GTP binding), Cdc42 and RhoA interact with the Sec3/Sec8 subunits of the exocyst complex in a mechanism that promotes the interaction of Sec3/Sec8 and the remaining subunits of the complex with IQGAP1.

Finally, we analyzed the contribution of Cdc42 and RhoA to matrix degradation of MDA cells. Knockdown of Cdc42 or RhoA in both MDA-MB-231 cells led to a drastic reduction of matrix degradation comparable with MT1-MMP depletion, whereas overall expression levels of MT1-MMP were not affected by knocking down Cdc42 or RhoA (Fig. S4, available at http://www.jcb.org/cgi/content/full/jcb.200709076/DC1). Of note, simultaneous depletion of both Cdc42 and RhoA with combined siRNA treatment led to a further decrease of degradation (unpublished data). All together, these results indicate that signaling pathways downstream of Cdc42 and RhoA are essential and probably act nonredundantly in the mechanism of invadopodial matrix degradation of MDA-MB-231 cells.

IQGAP1 and the exocyst complex are required for MT1-MMP accumulation at invadopodia

We first examined the distribution of Sec8 and IQGAP1 in MDA-MB-231 cells plated on fluorescent gelatin. Endogenous IQGAP1 was enriched at invadopodia of MDA-MB-231 cells together with filamentous actin (F-actin; Fig. 4 a). We could not analyze the distribution of the endogenous Sec8 (or Sec3) subunit in MDA-MB-231 cells because of the lack of good immunological reagents capable of detecting these proteins by immunofluorescence microscopy. Therefore, MDA-MB-231 cells were transfected with epitope-tagged Sec8 (V5 tagged) to facilitate detection. Besides a diffuse staining caused by accumulation in the cytosol, Sec8-V5 was also detected at invadopodia, where it colocalized with F-actin (Fig. 4 b). In addition, using MDA-MB-231 cells expressing an active mutant form of c-Src (Y527F), which triggers the appearance of larger, more stable invadopodia (Artym et al., 2006), we observed colocalization of endogenous IQGAP1 and Sec8-V5 at foci of degraded matrix (Fig. 4 c). Collectively, these data show that IQGAP1 and a component of the exocyst complex colocalize at invadopodia of MDA-MB-231 cells. Finally, as MT1-MMP has been shown to be specifically enriched at invadopodia (Monsky et al., 1993; Chen and Wang, 1999), one would expect cell surface MT1-MMP to colocalize with IQGAP1 and F-actin at invadopodia. MDA-MB-231 cells plated on FITC-gelatin were analyzed for cell surface MT1-MMP and intracellular IQGAP1/F-actin by immunofluorescence microscopy. Puncta of cell surface MT1-MMP immunofluorescence colocalized with F-actin/IQGAP1-positive invadopodia lying on top of degraded gelatin (Fig. 5 a, arrows).

We further investigated the effect of knocking down IQGAP1 on MDA cells' capacity to degrade gelatin. Depletion of IQGAP1 with two independent siRNAs to ∼30% of control levels in MDA-MB-231 cells (Fig. 5 b) resulted in a significant reduction of matrix degradation comparable with the effect of Sec8 depletion (Fig. 5 c), whereas overall levels of MT1-MMP in the different cell populations were similar (Fig. 5 b). The contribution of IQGAP1 and exocyst to the function of invadopodia was assessed by scoring the number of proteolytically active invadopodia positive for cell surface MT1-MMP in Sec8 or IQGAP1-depleted cells in comparison with mock-treated cells. Depletion of Sec8 or IQGAP1 led to a significant reduction of cell surface MT1-MMP–positive invadopodia (Fig. 5 d), demonstrating that the function of the exocyst complex and IQGAP1 is required for cell surface accumulation of MT1-MMP at invadopodia for invadopodia formation and activity.

The exocyst-binding domain of IQGAP1 is required for the mechanism of invadopodial proteolysis

To connect IQGAP1 and exocyst complex function at invadopodia, we made use of the IQGAP1-T1052AX2 (IQGAP1-T) protein (Fig. 6 a). This mutant form of IQGAP1, which is defective for binding to GTP-Cdc42/Rac1 (Fig. 3 b), has been shown to promote the extension of multiple lamellipodial structures in fibroblastic cell lines and, thus, is thought to represent a constitutively active form of IQGAP1 (Fukata et al., 2002). When expressed
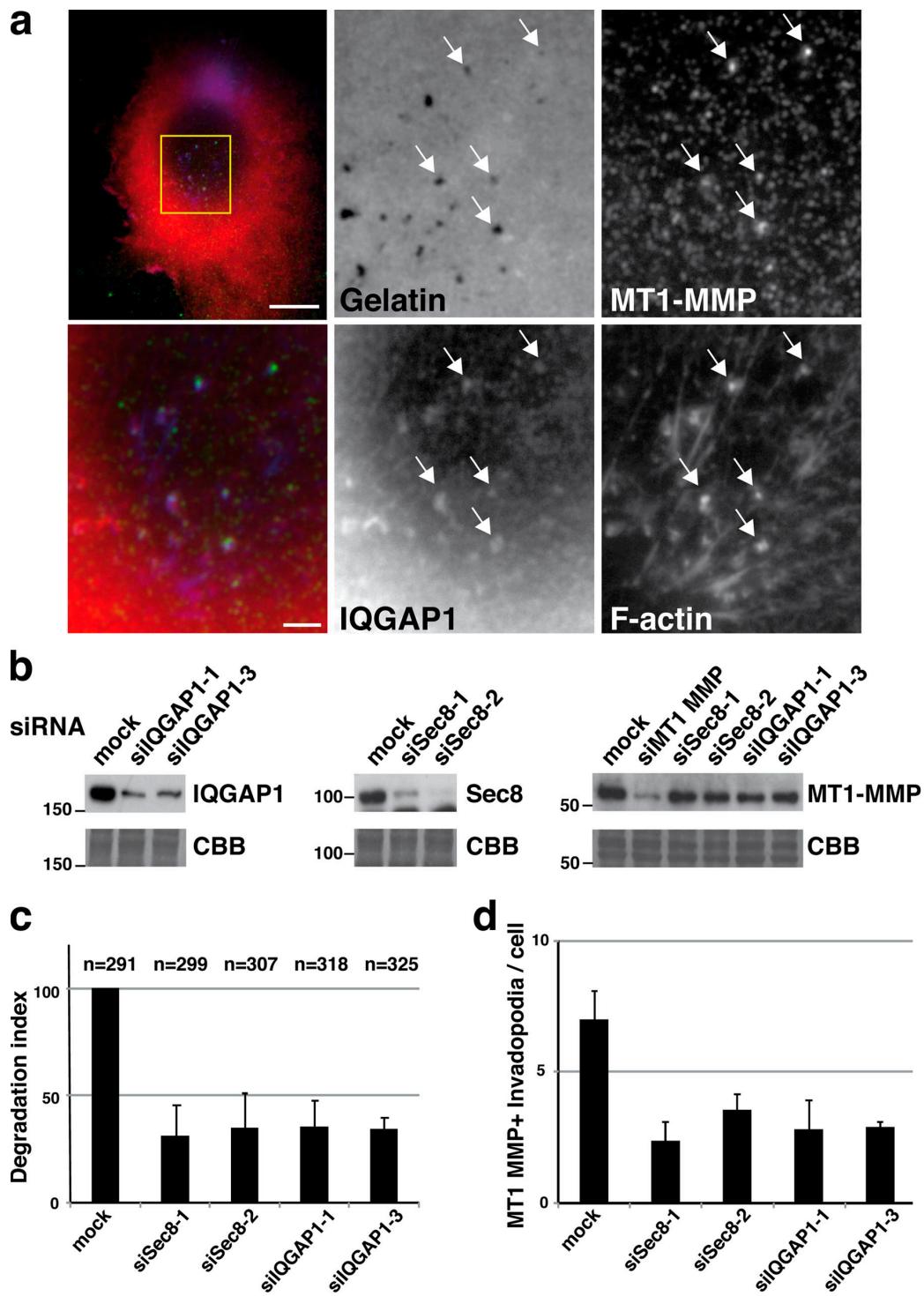
Figure 5. **IQGAP1 and Sec8 are required for invadopodial proteolysis of the matrix and MT1-MMP accumulation at invadopodia.** (a) MDA-MB-231 cells were plated on fluorescent FITC-gelatin for 6 h, subjected to surface labeling using anti–MT1-MMP antibody, fixed with PFA, and then permeabilized and stained for F-actin and endogenous IQGAP1. IQGAP1, red; MT1-MMP, green; F-actin, blue. The bottom left panel corresponds to the boxed area in the top panel. Black and white panels show individual images for surface-labeled MT1-MMP, IQGAP1, and F-actin that are all merged in the bottom left panel as well as FITC-gelatin. Of note, the punctuate accumulation of cell surface MT1-MMP at invadopodia was clearly detected by anti–MT1-MMP antibody over unspecific labeling of the gelatin (which appears as small dots visible even in regions of the gelatin free of cells; not depicted). Arrows indicate surface-labeled MT1-MMP at invadopodia on top of areas with various degrees of matrix degradation. Bars: (top) 2 μm; (bottom) 10 μm. (b) Expression levels of IQGAP1, Sec8, and MT1-MMP in MDA-MB-231 cells treated with specific siRNAs as indicated. Membranes were stained with Coomassie Brilliant blue (CBB) to control for equal loading. Molecular masses are indicated in kilodaltons. (c) Effect of IQGAP1 or Sec8 knockdown on matrix degradation of MDA-MB-231 cells. Degradation indexes calculated as in Fig. 1 a represent the mean ± SEM (error bars) of three independent experiments. The number of cells analyzed in each dataset is indicated on top of the graph. All siRNA-treated cell populations are significantly different as compared with mock-treated cells (P ≤ 0.01). (d) For each siRNA, matrix-degrading cells were scored for the presence of invadopodia, which were defined as surface-labeled MT-MMP accumulations lying on spots of degraded gelatin. Values are given as number ± SEM of MT1-MMP–positive invadopodia per cell from three independent experiments. All siRNA-treated cell populations are significantly different as compared with mock-treated cells (P ≤ 0.01).
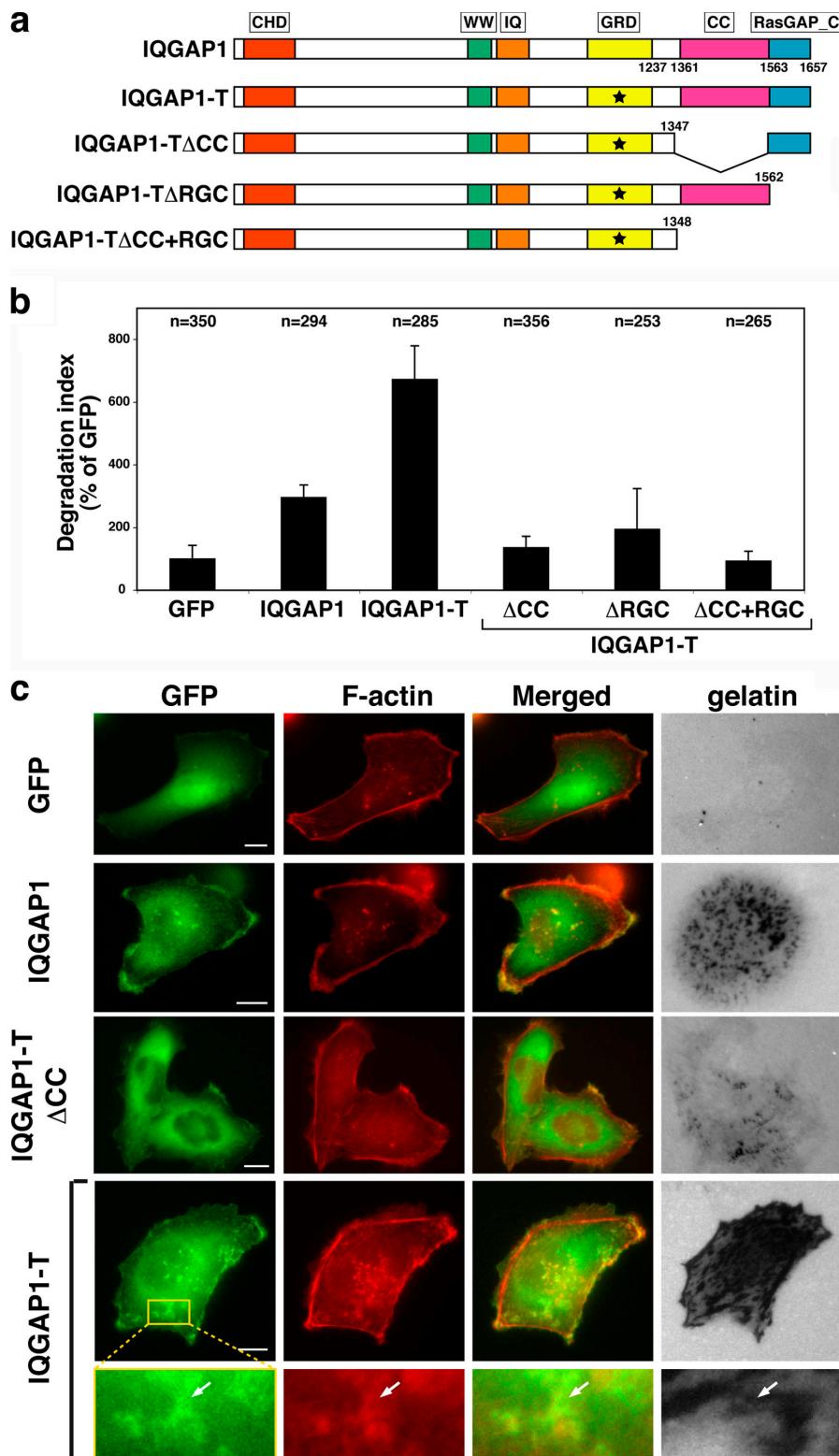
Figure 6. **Stimulation of invadopodial proteolysis by a constitutively active IQGAP1 mutant requires the Sec3/Sec8-binding domain.** (a) Schematic representation of IQGAP1, IQGAP1-T1050AX2 (IQGAP1-T) mutant, and its C-terminal deletion mutants. CHD, calponin homology domain; WW, polyproline-binding domain; IQ, calmodulin-binding motif; GRD, Ras GTPase-activating protein–related domain; CC, predicted coiled-coil domain; RasGAP_C, RasGAP C terminus. The stars indicate mutations in the GRD domain, which abolish binding to GTP-Cdc42/Rac1 (Fukata et al., 2002). (b) Evaluation of fluorescent matrix degradation in MDA-MT1ch cells transfected for 24 h with the indicated constructs and analyzed after 4 h of incubation on AlexaFluor350-labeled gelatin. Data are represented as normalized degradation (degradation index), calculated as the area of degraded matrix per cell relative to GFP-expressing cells (mean ± SEM [error bars] from three independent experiments). The number of cells analyzed for each construction is indicated above the graph. (c) Localization of IQGAP1 and IQGAP1-T to invadopodia. After 4 h on AlexaFluor350-labeled gelatin, MDA-MT1ch cells transfected with the indicated construct were fixed and processed for immunofluorescence analysis by staining with AlexaFluor633-phalloidin to visualize polymerized actin. GFP-tagged IQGAP1 proteins localize at F-actin–rich invadopodia lying on top of degraded areas of the fluorescent gelatin matrix (arrows). In contrast, the localization of GFP-IQGAP1-TΔCC appears more diffuse. Higher magnification views of the boxed area are shown. Bars, 10 μm.

in MDA-MT1ch cells, IQGAP1-T induced a striking 6.7-fold (±1) increase of matrix degradation (Fig. 6 b). Overexpression of WT IQGAP1 had a less stimulatory effect (×2.9 ± 0.4-fold). Distribution of the IQGAP1-WT and -T constructs was examined in MDA-MT1ch cells with respect to invadopodia localization. Like the endogenous proteins, both constructs were detected at the cell edge, where they colocalized with F-actin in cortical

bundles and at the ventral cell surface within invadopodia, coinciding with dark spots of degraded gelatin (Fig. 6 c). Importantly, deletion of the entire C-terminal region of IQGAP1-T (ΔCC + RGC [RasGAP C terminus]) or only the region of IQGAP1-T encompassing the Sec3/Sec8 binding domain (ΔCC) completely abolished the stimulatory effect of the activated mutant (Fig. 6, a and b). Noticeably, the distribution of IQGAP1-TΔCC
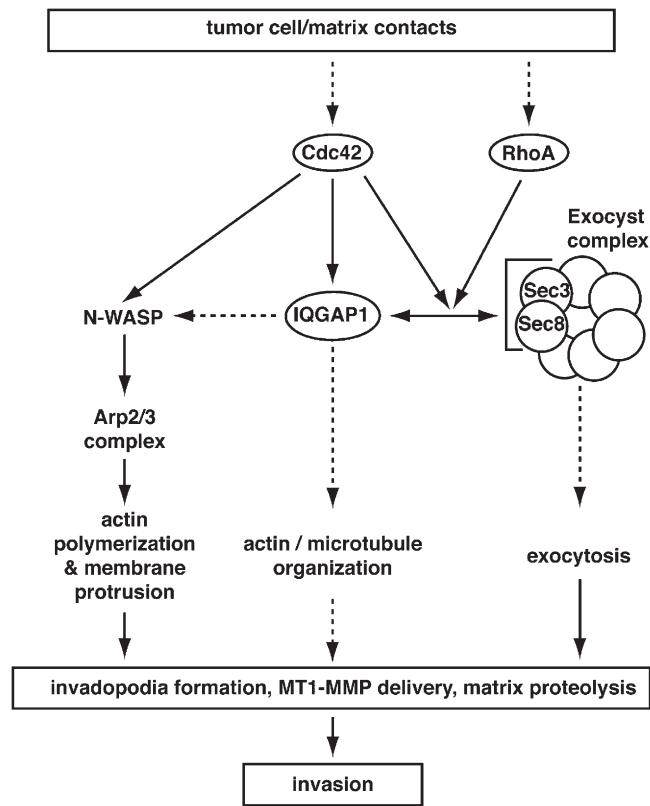
Figure 7. **Model for Rho-GTPase signaling control of invadopodial formation and function.** In response to the interaction of tumor cells with their 3D matrix environment, Rho-GTPases are activated locally, triggering actin assembly through activation of the Arp2/3 complex and leading to invadopodia protrusion within the ECM. IQGAP1, which is downstream of Cdc42 and RhoA, plays a central role in invadopodia function through the coordination of actin assembly with the exocytic machinery via the vesicle-docking exocyst complex and possibly through microtubule plus end anchoring (see Discussion for details).

appeared more diffuse, with no clear enrichment in ventral puncta (Fig. 6 c). In addition, we observed that IQGAP1-T deleted of its far-most C-terminal region (ΔRGC) also lost the capacity to stimulate matrix degradation, as it failed to promote lamellipodia formation in the initial study of Fukata et al., 2002 (see Discussion below). Of note, when expressed together with Sec8-HA and activated Cdc42 in HEK293 cells, IQGAP1-TΔCC could still be coimmunoprecipitated together with Sec8. We believe that this interaction likely represents the oligomerization of IQGAP1-TΔCC with endogenous IQGAP1 (Fukata et al., 1997; Ren et al., 2005), providing a bridge to the exocyst complex. At this stage, the relevance of IQGAP1 oligomerization to the mechanism of matrix degradation at invadopodia is not known. In any case, our data demonstrate that a constitutively active form of IQGAP1 has the capacity to stimulate invadopodia-mediated proteolysis of the matrix and that this activity requires the integrity of the C-terminal region of IQGAP1, including the exocyst complex–binding site.

Discussion

Several studies, including work from our laboratory, have demonstrated that the exocyst complex is involved in protein and membrane recycling in an evolutionarily conserved pathway used by surface proteins that have been internalized into endosomes and are returned back to specialized domains of the plasma membrane (Folsch et al., 2003; Prigent et al., 2003; Langevin et al., 2005). Various studies also identified endocytosis and recycling as a mechanism for controlling the activity of MT1-MMP during matrix degradation and invasion of tumor cells (Jiang et al., 2001; Uekita et al., 2001; Zucker et al., 2002; Remacle et al., 2003; Wu et al., 2005; Lafleur et al., 2006). Based on our findings that IQGAP1 and the exocyst complex, probably acting in a complex at invadopodia, are required for MT1-MMP accumulation at invadopodia, for invadopodial degradation of the matrix, and for invasion of breast carcinoma cells, we propose the model depicted in Fig. 7. In this scenario, the interaction of Sec3/Sec8 with IQGAP1 under the control of Cdc42/RhoA would provide a mechanism for targeting the exocyst complex to IQGAP1-enriched invadopodia of tumor cells. After targeting and/or assembly at invadopodia, the exocyst would facilitate tethering and polarized exocytosis of transport vesicles, resulting in delivery and accumulation of MT1-MMP at invadopodia. Noticeably, we observed a reduction of ventral puncta of F-actin and cortactin in cells depleted for Sec8 or IQGAP1 (unpublished data). However, whether this steady-state reduction reflects a general inhibition of invadopodia formation or the formation of more short-lived structures in the absence of IQGAP1 or the exocyst complex is unknown. In any case, our data support the view that the local activation of Cdc42 and RhoA at contact sites between tumor cells and the matrix would be required to interface proteins involved in cytoskeletal organization with proteins involved in exocytosis to assemble an active structure competent for matrix proteolysis and remodeling.

In addition, we found not only invadopodial proteolytic activity but also the mechanism of invadopodia formation to be critically dependent on expression of MT1-MMP (Figs. 1 b and S5). These observations are in agreement with recent studies showing that knockdown or pharmacological inhibition of MT1-MMP inhibits matrix degradation and invadopodia formation in carcinoma cells, including MDA-MB-231 cells (Artym et al., 2006; Clark et al., 2007). All together, these findings support the idea that MT1-MMP is not only the main proteolytic activity of invadopodia, but it also represents one prominent component of the building foundation of this structure.

Our study attributes a novel function to IQGAP1 as a key component of invadopodia. IQGAP1 localizes at lamellipodia of migratory cells, where it links microtubule plus ends to the actin cytoskeleton and, thereby, appears as a key regulator of cell polarity during migration (Noritake et al., 2005; Brown and Sacks, 2006). In addition, recent studies showing that IQGAP1 is overexpressed at invasive fronts of metastatic human colorectal carcinomas and enhances tumorigenesis of human breast epithelial cells all support an essential role for IQGAP1 in invasion and metastasis (Clark et al., 2000; Nabeshima et al., 2002; Mataraza et al., 2003; Jadeski et al., 2008). Our finding that IQGAP1 is enriched at invadopodia and that loss of its expression leads to a reduction of invadopodia function in matrix degradation provides a mechanism for IQGAP1's role in the dissemination of invasive carcinoma cells. IQGAP1 is a scaffolding protein involved in

multiple interactions with various cellular machineries. Besides its capacity to interact with the exocyst complex revealed by this study and, thus, the possibility to contribute to the delivery of invadopodial components, another function for IQGAP1 during invadopodia formation could be the stimulation of actin assembly by activation of a Neural Wiskott-Aldrich syndrome protein–Arp2/3 complex pathway known to control actin-driven invadopodial extension (Fig. 7; Yamaguchi et al., 2005a; Le Clainche et al., 2007). Another aspect of IQGAP1 activity at invadopodia may reside in its ability to capture microtubule plus ends via the formation of tripartite complexes with activated Cdc42 and microtubule-associated proteins CLIP-170 and adenomatous polyposis coli (Fukata et al., 2002; Watanabe et al., 2004). Microtubules and microtubule motors are important for the formation and dynamics of invadopodia-like structures of monocyte-derived cells called podosomes (Kopp et al., 2006). Whether invadopodia formation and/or activity similarly involves the microtubule network is presently unknown. Our observation that stimulation of invadopodial activity by constitutively active IQGAP1-T requires the CLIP170/adenomatous polyposis coli C-terminal binding domain of IQGAP1 suggests that this may indeed be the case and will require further investigation.

The interaction of IQGAP1 with Sec3/Sec8 that we document here, although it is promoted by GTP-Cdc42/RhoA, does not require direct binding of the GTPases to the GRD domain (Ras GTPase-activating protein–related domain) of IQGAP1. One possibility, which is supported by our coimmunoprecipitation data, is that activated Cdc42/RhoA binds to the Sec3/Sec8 subunits of the exocyst complex, leading to their interaction with IQGAP1. In *Saccharomyces cerevisiae*, GTP-bound Cdc42p and Rho1p interact directly with the N-terminal domain of Sec3p (Guo et al., 2001; Zhang et al., 2001). However, mammalian Sec3 has only weak homologies with yeast Sec3p within the Rho-binding domain (Matern et al., 2001). It should also be noticed that the counterpart of IQGAP1 in yeast, called Iqg1p (or Cyk1p), binds to and is required for the localization of Sec3p to the site of polarized growth (Osman et al., 2002). So far, our attempts to pull down purified recombinant N-terminal fragments of Sec3 or Sec8 with immobilized GTP-Cdc42 failed (unpublished data). Whether the binding site of GTP-Cdc42/RhoA on the mammalian exocyst complex is provided by the Sec3 or Sec8 subunit solely or by the Sec3/Sec8 interface or even a more complex interface consisting of Sec3/Sec8 in association with other exocyst subunits will require further study.

Our data indicate that the activity of both Cdc42 and RhoA is required for promoting the association between IQGAP1 and the exocyst complex and that these two Rho GTPases are involved in separate nonredundant functions during the mechanism of invadopodial proteolysis of the matrix. Rho proteins, which are well-known modulators of cytoskeletal changes that occur during cell migration, contribute to various aspects of tumorigenesis, including invasion of highly motile carcinoma cells (Sahai and Marshall, 2002). This role in invasion is correlated with the altered expression of Rho GTPases and some of their regulators and effectors in various human tumors, particularly the most aggressive and metastatic forms of cancers (Fritz et al., 2002; Sahai, 2005). Along this line, Cdc42

has been shown to control the formation of invadopodia in human melanoma and rat mammary adenocarcinoma tumor cell lines based on a Neural Wiskott-Aldrich syndrome protein–Arp2/3 complex signaling activation cascade (Nakahara et al., 2003; Yamaguchi et al., 2005a). A large body of work also implicates RhoA-related proteins (RhoA, RhoB, and RhoC) and downstream signaling pathways in the progression and invasion of tumors of various origins (Fritz et al., 2002; Sahai and Marshall, 2002; Pille et al., 2005; Wyckoff et al., 2006). Our study implicating RhoA in invadopodial matrix degradation extends previous studies showing that RhoA is required for the formation and activity of podosome/invadopodia-like invasive structures in v-Src–transformed fibroblasts (Berdeaux et al., 2004; for reviews see Linder and Aepfelbacher, 2003; Jurdic et al., 2006). The picture that is thus emerging collectively from these previous studies and our work connecting Cdc42/RhoA with the vesicle-tethering machinery implies that the role of Cdc42/RhoA at invadopodia is not restricted to actin assembly but rather involves the coordination of cytoskeleton remodeling with vesicle docking/exocytosis for the generation of protrusions and for invasiveness.

Materials and methods

Plasmid constructions
To obtain expression vectors coding for human Sec3, Sec8, Exo70, and Exo84 C-terminally tagged with V5 or HA tag, ORFs were amplified by PCR and cloned into pcDNA3.1D/V5-His-TOPO (Invitrogen). Alternatively, PCRs were performed with reverse primers, including the sequence for HA tag (5'-TACCCATACGATGTTCCAGATTACGCTTAA-3'), and fragments were cloned into pcDNA3.1 (Invitrogen). HA-tagged subfragments of Sec3 and Sec8 were obtained by PCR and subcloned in pcDNA3.1. Full-length ORF of exocyst subunits (Sec3, Sec8, Exo70, and Exo84) were subcloned into the yeast two-hybrid bait plasmid pB27 derived from the original pBTM116 plasmid (Formstecher et al., 2005). GFP-IQGAP1 and -IQGAP1-T1050AX2 expression constructs were gifts from K. Kaibuchi (Nagoya University, Nagoya, Japan). IQGAP1-T1050AX2 (IQGAP1-T) harbors a substitution of Thr/Val/Ile (aa 1,050–1,052) to Ala/Ala/Ala and a tandem duplication of region aa 1,043–1,059 (Fukata et al., 2002). Expression vectors encoding for IQGAP1 C-terminal fragments fused with GST were generated by PCR and cloned into pGEX-4T-1 (GE Healthcare). C-terminal deletion mutants of GFP-IQGAP1-T1050AX2 were constructed as follows: ΔCC, a fragment corresponding to aa 1,563–1,657, was amplified by PCR and inserted into pEGFP-IQGAP1-T1050AX2 between an internal SwaI site (corresponding to aa position 1,347) and a SacII site of the 3'-end multiple cloning site fusing aa 1–1,374 with 1,563–1,657; ΔRGC, a fragment corresponding to aa 1–1,562, was amplified by PCR and cloned into the SalI–SacII sites of pEGFP-C3; ΔCC + RGC and pEGFP-IQGAP1-T1050AX2 were cleaved at SwaI (internal) and SmaI 3'-end multiple cloning sites and were self-ligated.

Human MT1-MMP cDNA was obtained from RZPD GmbH (clone numbers IRAKp961P20107QQ2 and IRAKp961O0484QQ2). MT1-MMP–mCherry was generated by PCR using the same strategy, resulting in the insertion of mCherry (a gift from R.Y. Tsien, University of California, San Diego, La Jolla, CA) between aa 534 and 535, N terminal to the transmembrane region. Expression vectors for myc-tagged Cdc42, Rac1, and RhoA mutant forms were gifts from A. Hall (University College London, London, UK). To obtain GFP-JIP3-LZII expression vector, a JIP3 fragment corresponding to aa 371–507 was amplified by PCR and inserted into the XhoI–EcoRI sites of pEGFP-C3.

Cell culture
Unless specified, reagents were obtained from Invitrogen. MDA-MB-231 human breast adenocarcinoma cells were obtained from the European Collection of Cell Cultures and were cultured in L-15 medium (Sigma-Aldrich) supplemented with 2 mM glutamine and 15% FCS. To generate MDA-MB-231 cells stably expressing MT1-MMP–mCherry, cells were transfected with Lipofectamine 2000 (Invitrogen) and selected with 800 µg/ml geneticin,

and mCherry-positive cells were sorted by flow cytometry with FACSAria (BD Biosciences). MDA-MT1ch cells were maintained in medium supplemented with 500 μg/ml geneticin. HEK293 and HeLa cells were maintained in DME supplemented with 10% FCS, penicillin, and streptomycin.

Antibodies and reagents

Mouse monoclonal antibody against MT1-MMP (clone 2D7; Chenard et al., 1999) was a gift from M.C. Rio (Institut de Génétique et de Biologie Moléculaire et Cellulaire, Illkirch, France). Monoclonal mouse anti-GFP (mixture of clone 7.1 and 13.1) and rat anti-HA (clone 3F10) antibodies were purchased from Roche. Monoclonal mouse anti-myc tag (clone 9E10) was purified on protein G–Sepharose. Monoclonal mouse anti-V5 was purchased from Invitrogen. Monoclonal mouse anti-Sec8 (clone 14) and anti-Sec6 (clone 9H5) antibodies were obtained from BD Biosciences and Nventa, respectively. Rabbit polyclonal anti-Sec10 antibodies have been previously described (Prigent et al., 2003). Monoclonal (clone AF4) and polyclonal anti-IQGAP1 (H-190) antibodies were obtained from Millipore and Santa Cruz Biotechnology, Inc., respectively. Monoclonal anti-RhoA (clone 26C4) was provided by J. Bertoglio (Institut National de la Santé et de la Recherche Médicale, Unite 461, Chatenay-Malabry, France). Monoclonal anti-Cdc42 (clone 44) antibody was purchased from BD Biosciences. Monoclonal anticortactin antibody (clone 4F11) was obtained from Millipore. AlexaFluor-labeled phalloidin and anti–mouse IgG antibodies were purchased from Invitrogen. HRP-conjugated anti–rat IgG antibodies were purchased from GE Healthcare. HRP-conjugated anti–mouse IgG, Cy3-conjugated F(ab')2 anti–rabbit, and anti–mouse IgG antibodies were obtained from Jackson ImmunoResearch Laboratories.

Yeast two-hybrid assay

The yeast two-hybrid screens were performed using the Sec3, Sec8, Exo70, and Exo84 exocyst subunits as baits to screen a human placenta random-primed cDNA library using a previously described mating protocol (Formstecher et al., 2005).

GST pull-down assay

GST-IQGAP1 fusion proteins expressed in *Escherichia coli* (BL21 DE3) were purified using glutathione–Sepharose 4B (GE Healthcare). GST-IQGAP1 fusion proteins or 2 μM GST was incubated with 500 μg of total protein of HeLa cells extracted in binding buffer (50 mM Tris-HCl, pH 7.5, 137 mM NaCl, 1% Triton X-100, 10 mM MgCl$_2$, and 10% glycerol) supplemented with protease inhibitors (Complete EDTA free; Roche) and 0.5% BSA. Then, 30 μl of 50% glutathione bead slurry was added and further incubated for 60 min at 4°C. Beads were washed four times with binding buffer, and bound proteins were eluted in SDS sample buffer, separated by SDS-PAGE, and detected by immunoblotting with the indicated antibodies.

For GST pull-down assays using in vitro–synthesized proteins, biotin-labeled in vitro–translated proteins were synthesized by TNT T7 Quick Coupled Transcription/Translation System and Transcend NonRadioactive Translation Detection systems (Promega). GST-IQGAP1 fusion proteins or 2 μM GST was incubated with 10 μl of in vitro–synthesized biotin-labeled protein for 30 min at 4°C in 300 μl of the aforementioned binding buffer supplemented with protease inhibitors and 0.5% BSA. Then, 30 μl of 50% glutathione bead slurry was added and further incubated for 60 min at 4°C. Beads were washed four times with binding buffer, and bound proteins were eluted in SDS sample buffer, separated by SDS-PAGE, and detected with streptavidin-HRP (Thermo Fisher Scientific).

Immunoprecipitation

HEK293 cells were transfected using FuGENE 6 (Roche). 24 h after transfection, cells were lysed in lysis buffer (50 mM Tris-HCl, pH 7.5, 150 mM NaCl, 1% Triton X-100, and 1 mM EDTA) with protease inhibitors and centrifuged at 13,000 rpm for 10 min at 4°C. Supernatants (1–2 mg of total proteins in 1 ml) were incubated with 1 μg of antibody for 30 min at 4°C, and then protein A or protein G Sepharose 4 Fast Flow (GE Healthcare) was added and further incubated for 1 h at 4°C. Beads were washed three times in lysis buffer, and bound proteins were eluted in SDS sample buffer, separated by SDS-PAGE, and detected by immunoblotting analysis with the indicated antibodies using Lumi-Light[PLUS] substrate (Roche).

siRNA and plasmid transfection

Lipofectamine 2000 was used for transfection of MDA-MB-231 cells with expression vectors, and cells were assayed 24 h later. For siRNA treatment, MDA-MB-231 cells were transfected with 50–200 nM of specific siRNA duplex with Oligofectamine (Invitrogen) according to the manufacturer's

instructions (see Table S1 for a list of the different siRNAs used in this study; available at http://www.jcb.org/cgi/content/full/jcb.200709076/DC1). Cells were assayed after 72 h of treatment.

Fluorescent gelatin degradation assay

FITC-labeled gelatin was obtained from Invitrogen. AlexaFluor350-conjugated gelatin was prepared by labeling porcine gelatin with AlexaFluor350 (Invitrogen) according to the manufacturer's instructions. Coverslips coated with fluorescent gelatin were prepared as described by Artym et al. (2006). In brief, coverslips (18-mm diameter) were coated with 0.5 μg/ml (MDA-MB-231 cells) or 50 μg/ml poly-ʟ-lysine (MDA-MT1ch cells) for 20 min at room temperature, washed with PBS, and fixed with 0.5% glutaraldehyde (Sigma-Aldrich) for 15 min. After three washes, the coverslips were inverted on an 80-μl drop of 0.2% fluorescently labeled gelatin in 2% sucrose in PBS and incubated for 10 min at room temperature. After washing with PBS, coverslips were incubated in 5 mg/ml sodium borohydride for 3 min, washed three times in PBS, and finally incubated in 2 ml of complete medium for a minimum of 2 h before adding the cells.

To assess the ability of cells to form invadopodia and degrade the matrix, 7×10^4 cells/12 wells were plated on fluorescent gelatin-coated coverslips and incubated at 37°C for 4–6 h as indicated. Cells were then fixed with 4% PFA for 20 min, quenched with 50 mM NH$_4$Cl for 10 min, permeabilized with 0.2% saponin for 5 min, and processed for intracellular immunofluorescence labeling with AlexaFluor-phalloidin as indicated. Cells were imaged with 40× or 63× objectives of a wide-field microscope (DM6000 B/M; Leica) equipped with a CCD camera (CoolSNAP HQ; Photometrics). For quantification of degradation, the total area of degraded matrix in one field (black pixels) measured using the Threshold command of MetaMorph 6.2.6 (MDS Analytical Technologies) was divided by the total number of phalloidin-labeled cells in the field to define a degradation index.

MT1-MMP cell surface immunofluorescence

For labeling of cell surface MT1-MMP, after incubation on fluorescent gelatin as described in the previous section, cells were further incubated on ice for 30 min with anti–MT1-MMP mAb in PBS containing 10% FCS. Then, cells were fixed and permeabilized with 4% PFA and permeabilized with 0.2% saponin as described above and labeled with AlexaFluor-phalloidin and antibodies specific for invadopodial markers as indicated. Cells were imaged with the 100× objective of a wide-field DM6000 B/M microscope equipped with a CoolSNAP HQ CCD camera.

Matrigel invasion assay

Matrigel invasion inserts and control (without matrigel) inserts (8-μm pores) for 24-well tissue culture plates were purchased from BD Biosciences. In brief, matrigel invasion inserts (top chambers) were rehydrated for 2 h at 37°C in culture medium. Then, both rehydrated matrigel invasion and control inserts were placed in bottom chambers containing culture medium supplemented with 20 ng/ml hepatocyte growth factor (EMD) as chemo-attractant. MDA-MB-231 cells were transfected with siRNA for 72 h and detached, and 2×10^4 cells were added into the top chambers and incubated at 37°C for 18 h. Cells that had not migrated were thoroughly removed from the upper surface of the insert membrane with a cotton swab. Inserts were then washed with PBS, and cells were fixed with 4% PFA in PBS for 20 min and stained with 0.1% crystal violet (Bio-Rad Laboratories), 200 mM MES (MP Biomedicals), pH 6.0, for 10 min. Inserts were washed twice with water and allowed to air dry. Membranes were then scanned with a scanner (Perfection 3200 Photo; Epson) at maximal resolution (6,400 dpi) and analyzed with multidimensional image analysis segmentation software to count the number of cells present on the membranes. This software uses wavelet decomposition to detect cells based on their homogeneous morphology on the scanned images, even when the background is not homogeneous. To allow better cell separation in aggregates, a watershed operator is applied in the wavelet maps. To obtain the invasion index, the number of cells that had migrated through the matrigel was divided by the number of cells that had migrated in the control inserts without matrigel. The invasion index of mock-treated cells was set as 100%.

Online supplemental material

Fig. S1 presents a summary of yeast two-hybrid and GST pull-down interactions of IQGAP with the exocyst complex subunits. Fig. S2 shows an interaction of in vitro–translated exocyst subunits with C-terminal fragments of IQGAP1 and mapping of the IQGAP1-binding region of Sec3 and Sec8. Fig. S3 shows that activated Cdc42 promotes IQGAP1 association with Sec3 in transfected HEK293 cells. Fig. S4 shows that Cdc42 and RhoA are

required for matrix degradation of MDA-MB-231 cells. Fig. S5 shows that loss of MT1-MMP expression inhibits invadopodia formation in MDA-MB-231 cells. Table S1 presents the siRNAs used in this study. Online supplemental material is available at http://www.jcb.org/cgi/content/full/jcb.200709076/DC1.

References

Artym, V.V., Y. Zhang, F. Seillier-Moiseiwitsch, K.M. Yamada, and S.C. Mueller. 2006. Dynamic interactions of cortactin and membrane type 1 matrix metalloproteinase at invadopodia: defining the stages of invadopodia formation and function. *Cancer Res.* 66:3034–3043.

Berdeaux, R.L., B. Diaz, L. Kim, and G.S. Martin. 2004. Active Rho is localized to podosomes induced by oncogenic Src and is required for their assembly and function. *J. Cell Biol.* 166:317–323.

Brown, M.D., and D.B. Sacks. 2006. IQGAP1 in cellular signaling: bridging the GAP. *Trends Cell Biol.* 16:242–249.

Buccione, R., J.D. Orth, and M.A. McNiven. 2004. Foot and mouth: podosomes, invadopodia and circular dorsal ruffles. *Nat. Rev. Mol. Cell Biol.* 5:647–657.

Chen, W.T., and J.Y. Wang. 1999. Specialized surface protrusions of invasive cells, invadopodia and lamellipodia, have differential MT1-MMP, MMP-2, and TIMP-2 localization. *Ann. NY Acad. Sci.* 878:361–371.

Chenard, M.P., Y. Lutz, A. Mechine-Neuville, I. Stoll, J.P. Bellocq, M.C. Rio, and P. Basset. 1999. Presence of high levels of MT1-MMP protein in fibroblastic cells of human invasive carcinomas. *Int. J. Cancer.* 82:208–212.

Clark, E.A., T.R. Golub, E.S. Lander, and R.O. Hynes. 2000. Genomic analysis of metastasis reveals an essential role for RhoC. *Nature.* 406:532–535.

Clark, E.S., A.S. Whigham, W.G. Yarbrough, and A.M. Weaver. 2007. Cortactin is an essential regulator of matrix metalloproteinase secretion and extracellular matrix degradation in invadopodia. *Cancer Res.* 67:4227–4235.

Deryugina, E.I., and J.P. Quigley. 2006. Matrix metalloproteinases and tumor metastasis. *Cancer Metastasis Rev.* 25:9–34.

Folsch, H., M. Pypaert, S. Maday, L. Pelletier, and I. Mellman. 2003. The AP-1A and AP-1B clathrin adaptor complexes define biochemically and functionally distinct membrane domains. *J. Cell Biol.* 163:351–362.

Formstecher, E., S. Aresta, V. Collura, A. Hamburger, A. Meil, A. Trehin, C. Reverdy, V. Betin, S. Maire, C. Brun, et al. 2005. Protein interaction mapping: a *Drosophila* case study. *Genome Res.* 15:376–384.

Friedl, P., and K. Wolf. 2003. Tumour-cell invasion and migration: diversity and escape mechanisms. *Nat. Rev. Cancer.* 3:362–374.

Fritz, G., C. Brachetti, F. Bahlmann, M. Schmidt, and B. Kaina. 2002. Rho GTPases in human breast tumours: expression and mutation analyses and correlation with clinical parameters. *Br. J. Cancer.* 87:635–644.

Fukata, M., S. Kuroda, K. Fujii, T. Nakamura, I. Shoji, Y. Matsuura, K. Okawa, A. Iwamatsu, A. Kikuchi, and K. Kaibuchi. 1997. Regulation of cross-linking of actin filament by IQGAP1, a target for Cdc42. *J. Biol. Chem.* 272:29579–29583.

Fukata, M., T. Watanabe, J. Noritake, M. Nakagawa, M. Yamaga, S. Kuroda, Y. Matsuura, A. Iwamatsu, F. Perez, and K. Kaibuchi. 2002. Rac1 and Cdc42 capture microtubules through IQGAP1 and CLIP-170. *Cell.* 109:873–885.

Grindstaff, K.K., C. Yeaman, N. Anandasabapathy, S.C. Hsu, E. Rodriguez-Boulan, R.H. Scheller, and W.J. Nelson. 1998. Sec6/8 complex is recruited to cell-cell contacts and specifies transport vesicle delivery to the basal-lateral membrane in epithelial cells. *Cell.* 93:731–740.

Guo, W., F. Tamanoi, and P. Novick. 2001. Spatial regulation of the exocyst complex by Rho1 GTPase. *Nat. Cell Biol.* 3:353–360.

Hashimoto, S., Y. Onodera, A. Hashimoto, M. Tanaka, M. Hamaguchi, A. Yamada, and H. Sabe. 2004. Requirement for Arf6 in breast cancer invasive activities. *Proc. Natl. Acad. Sci. USA.* 101:6647–6652.

Hotary, K., X.-Y. Li, E. Allen, S.L. Stevens, and S.J. Weiss. 2006. A cancer cell metalloprotease triad regulates the basement membrane transmigration program. *Genes Dev.* 20:2673–2686.

Hsu, S.C., D. TerBush, M. Abraham, and W. Guo. 2004. The exocyst complex in polarized exocytosis. *Int. Rev. Cytol.* 233:243–265.

Itoh, Y., and M. Seiki. 2006. MT1-MMP: a potent modifier of pericellular microenvironment. *J. Cell. Physiol.* 206:1–8.

Jadeski, L., J.M. Mataraza, H.-W. Jeong, Z. Li, and D.B. Sacks. 2008. IQGAP1 stimulates proliferation and enhances tumorigenesis of human breast epithelial cells. *J. Biol. Chem.* 283:1008–1017.

Jiang, A., K. Lehti, X. Wang, S.J. Weiss, J. Keski-Oja, and D. Pei. 2001. Regulation of membrane-type matrix metalloproteinase 1 activity by dynamin-mediated endocytosis. *Proc. Natl. Acad. Sci. USA.* 98:13693–13698.

Jurdic, P., F. Saltel, A. Chabadel, and O. Destaing. 2006. Podosome and sealing zone: specificity of the osteoclast model. *Eur. J. Cell Biol.* 85:195–202.

Kelkar, N., S. Gupta, M. Dickens, and R.J. Davis. 2000. Interaction of a mitogen-activated protein kinase signaling module with the neuronal protein JIP3. *Mol. Cell. Biol.* 20:1030–1043.

Kopp, P., R. Lammers, M. Aepfelbacher, G. Woehlke, T. Rudel, N. Machuy, W. Steffen, and S. Linder. 2006. The kinesin KIF1C and microtubule plus ends regulate podosome dynamics in macrophages. *Mol. Biol. Cell.* 17:2811–2823.

Lafleur, M.A., F.A. Mercuri, N. Ruangpanit, M. Seiki, H. Sato, and E.W. Thompson. 2006. Type I collagen abrogates the clathrin-mediated internalization of membrane type 1 matrix metalloproteinase (MT1-MMP) via the MT1-MMP hemopexin domain. *J. Biol. Chem.* 281:6826–6840.

Langevin, J., M.J. Morgan, J.B. Sibarita, S. Aresta, M. Murthy, T. Schwarz, J. Camonis, and Y. Bellaiche. 2005. *Drosophila* exocyst components Sec5, Sec6, and Sec15 regulate DE-cadherin trafficking from recycling endosomes to the plasma membrane. *Dev. Cell.* 9:355–376.

Le Clainche, C., D. Schlaepfer, A. Ferrari, M. Klingauf, K. Grohmanova, A. Veligodskiy, D. Didry, D. Le, C. Egile, M.-F. Carlier, and R. Kroschewski. 2007. IQGAP1 stimulates actin assembly through the N-Wasp-Arp2/3 pathway. *J. Biol. Chem.* 282:426–435.

Linder, S., and M. Aepfelbacher. 2003. Podosomes: adhesion hot-spots of invasive cells. *Trends Cell Biol.* 13:376–385.

Mataraza, J.M., M.W. Briggs, Z. Li, A. Entwistle, A.J. Ridley, and D.B. Sacks. 2003. IQGAP1 promotes cell motility and invasion. *J. Biol. Chem.* 278:41237–41245.

Matern, H.T., C. Yeaman, W.J. Nelson, and R.H. Scheller. 2001. The Sec6/8 complex in mammalian cells: characterization of mammalian Sec3, subunit interactions, and expression of subunits in polarized cells. *Proc. Natl. Acad. Sci. USA.* 98:9648–9653.

McNiven, M.A., M. Baldassarre, and R. Buccione. 2004. The role of dynamin in the assembly and function of podosomes and invadopodia. *Front. Biosci.* 9:1944–1953.

Monsky, W.L., T. Kelly, C.-Y. Lin, Y. Yeh, W.G. Stetler-Stevenson, S.C. Mueller, and W.-T. Chen. 1993. Binding and localization of Mr 72,000 matrix metalloproteinase at cell surface invadopodia. *Cancer Res.* 53:3159–3164.

Mueller, S.C., G. Ghersi, S.K. Akiyama, Q.X. Sang, L. Howard, M. Pineiro-Sanchez, H. Nakahara, Y. Yeh, and W.T. Chen. 1999. A novel protease-docking function of integrin at invadopodia. *J. Biol. Chem.* 274:24947–24952.

Munson, M., and P. Novick. 2006. The exocyst defrocked, a framework of rods revealed. *Nat. Struct. Mol. Biol.* 13:577–581.

Nabeshima, K., Y. Shimao, T. Inoue, and M. Koono. 2002. Immunohistochemical analysis of IQGAP1 expression in human colorectal carcinomas: its overexpression in carcinomas and association with invasion fronts. *Cancer Lett.* 176:101–109.

Nakahara, H., T. Otani, T. Sasaki, Y. Miura, Y. Takai, and M. Kogo. 2003. Involvement of Cdc42 and Rac small G proteins in invadopodia formation of RPMI7951 cells. *Genes Cells.* 8:1019–1027.

Noritake, J., T. Watanabe, K. Sato, S. Wang, and K. Kaibuchi. 2005. IQGAP1: a key regulator of adhesion and migration. *J. Cell Sci.* 118:2085–2092.

Osman, M.A., J.B. Konopka, and R.A. Cerione. 2002. Iqg1p links spatial and secretion landmarks to polarity and cytokinesis. *J. Cell Biol.* 159:601–611.

Pille, J.Y., C. Denoyelle, J. Varet, J.R. Bertrand, J. Soria, P. Opolon, H. Lu, L.L. Pritchard, J.P. Vannier, C. Malvy, et al. 2005. Anti-RhoA and anti-RhoC siRNAs inhibit the proliferation and invasiveness of MDA-MB-231 breast cancer cells in vitro and in vivo. *Mol. Ther.* 11:267–274.

Prigent, M., T. Dubois, G. Raposo, V. Derrien, D. Tenza, C. Rosse, J. Camonis, and P. Chavrier. 2003. ARF6 controls post-endocytic recycling through its downstream exocyst complex effector. *J. Cell Biol.* 163:1111–1121.

Remacle, A., G. Murphy, and C. Roghi. 2003. Membrane type I-matrix metalloproteinase (MT1-MMP) is internalised by two different pathways and is recycled to the cell surface. *J. Cell Sci.* 116:3905–3916.

Ren, J.-G., Z. Li, D.L. Crimmins, and D.B. Sacks. 2005. Self-association of IQGAP1: characterization and functional sequelae. *J. Biol. Chem.* 280:34548–34557.

Ren, X.D., and M.A. Schwartz. 2000. Determination of GTP loading on Rho. *Methods Enzymol.* 325:264–272.

Rosse, C., A. Hatzoglou, M.C. Parrini, M.A. White, P. Chavrier, and J. Camonis. 2006. RalB mobilizes the exocyst to drive cell migration. *Mol. Cell. Biol.* 26:727–734.

Sabeh, F., I. Ota, K. Holmbeck, H. Birkedal-Hansen, P. Soloway, M. Balbin, C. Lopez-Otin, S. Shapiro, M. Inada, S. Krane, et al. 2004. Tumor cell traffic through the extracellular matrix is controlled by the membrane-anchored collagenase MT1-MMP. *J. Cell Biol.* 167:769–781.

Sahai, E. 2005. Mechanisms of cancer cell invasion. *Curr. Opin. Genet. Dev.* 15:87–96.

Sahai, E., and C.J. Marshall. 2002. RHO-GTPases and cancer. *Nat. Rev. Cancer.* 2:133–142.

Sugihara, K., S. Asano, K. Tanaka, A. Iwamatsu, K. Okawa, and Y. Ohta. 2002. The exocyst complex binds the small GTPase RalA to mediate filopodia formation. *Nat. Cell Biol.* 4:73–78.

Tague, S.E., V. Muralidharan, and C. D'Souza-Schorey. 2004. ADP-ribosylation factor 6 regulates tumor cell invasion through the activation of the MEK/ERK signaling pathway. *Proc. Natl. Acad. Sci. USA.* 101:9671–9676.

TerBush, D.R., T. Maurice, D. Roth, and P. Novick. 1996. The exocyst is a multiprotein complex required for exocytosis in *Saccharomyces cerevisiae.* *EMBO J.* 15:6483–6494.

Ueda, J., M. Kajita, N. Suenaga, K. Fujii, and M. Seiki. 2003. Sequence-specific silencing of MT1-MMP expression suppresses tumor cell migration and invasion: importance of MT1-MMP as a therapeutic target for invasive tumors. *Oncogene.* 22:8716–8722.

Uekita, T., Y. Itoh, I. Yana, H. Ohno, and M. Seiki. 2001. Cytoplasmic tail-dependent internalization of membrane-type 1 matrix metalloproteinase is important for its invasion-promoting activity. *J. Cell Biol.* 155:1345–1356.

Watanabe, T., S. Wang, J. Noritake, K. Sato, M. Fukata, M. Takefuji, M. Nakagawa, N. Izumi, T. Akiyama, and K. Kaibuchi. 2004. Interaction with IQGAP1 links APC to Rac1, Cdc42, and actin filaments during cell polarization and migration. *Dev. Cell.* 7:871–883.

Wu, X., B. Gan, Y. Yoo, and J.L. Guan. 2005. FAK-mediated src phosphorylation of endophilin A2 inhibits endocytosis of MT1-MMP and promotes ECM degradation. *Dev. Cell.* 9:185–196.

Wyckoff, J.B., S.E. Pinner, S. Gschmeissner, J.S. Condeelis, and E. Sahai. 2006. ROCK- and myosin-dependent matrix deformation enables protease-independent tumor-cell invasion in vivo. *Curr. Biol.* 16:1515–1523.

Yamaguchi, H., M. Lorenz, S. Kempiak, C. Sarmiento, S. Coniglio, M. Symons, J. Segall, R. Eddy, H. Miki, T. Takenawa, and J. Condeelis. 2005a. Molecular mechanisms of invadopodium formation: the role of the N-WASP-Arp2/3 complex pathway and cofilin. *J. Cell Biol.* 168:441–452.

Yamaguchi, H., J. Wyckoff, and J. Condeelis. 2005b. Cell migration in tumors. *Curr. Opin. Cell Biol.* 17:559–564.

Zhang, X., E. Bi, P. Novick, L. Du, K.G. Kozminski, J.H. Lipschutz, and W. Guo. 2001. Cdc42 interacts with the exocyst and regulates polarized secretion. *J. Biol. Chem.* 276:46745–46750.

Zucker, S., M. Hymowitz, C.E. Conner, E.A. DiYanni, and J. Cao. 2002. Rapid trafficking of membrane type 1-matrix metalloproteinase to the cell surface regulates progelatinase a activation. *Lab. Invest.* 82:1673–1684.